



The Influence of Electrical Pulses on the Evolution Characteristics of Coal Pore Structure

Lu Chang, Juan Huang, Haofei Zheng

School of Resources and Environment, Henan Polytechnic University, Henan, China

ABSTRACT

China is rich in coalbed methane resources, comparable to conventional natural gas, with enormous development potential. However, low-permeability and low-pressure coal reservoirs are widespread, leading to generally low single-well production. This paper focuses on the coal samples from Zhangcun, Lu'an, and uses an independently developed high-voltage electric pulse fracturing platform to conduct high-voltage electric pulse fracturing experiments on coal bodies. Mercury pressure and liquid nitrogen adsorption techniques were employed to analyze changes in pore structure before and after fracturing. The conclusions are as follows: High-pressure mercury pressure test data show that after high-voltage electric pulse fracturing, the macroporosity and mesoporosity of the Zhangcun coal sample increase, along with their proportion of total pore volume, indicating that the electric pulse shock wave primarily affects the meso- and macroporosity of the coal body. Low-temperature liquid nitrogen adsorption data indicate that high-voltage electric pulse fracturing reduces the liquid nitrogen adsorption capacity of the Zhangcun coal sample, altering the internal pore morphology. The ink bottle pores in the Zhangcun coal sample are effectively modified after fracturing. Analysis of liquid nitrogen adsorption data shows that after high-voltage electric pulse fracturing, the average pore size of the mesopores in the Zhangcun coal sample increases, while the pore volume and specific surface area decrease, indicating that the modified coal sample exhibits pore transformation.

KEYWORDS

Coalbed methane; High voltage electric pulse; Pore structure characteristics.

1. INTRODUCTION

China's coal resources are relatively abundant, with large reserves. Coal is also an important industrial raw material and energy source, so it will continue to dominate energy consumption in the future^[1-3]. According to the "China Energy Development Report 2024," coal demand is increasing, with annual raw coal production estimated at about 4.78 billion tons, up 1.2% year-on-year. However, due to years of mining, the amount of shallow coal has become depleted, making it difficult to meet the needs of various industries, leading to an increase in mining depth each year. As mining depth increases, the pressure of coal seam gas also rises, resulting in greater gas outflow, posing serious safety hazards^[4-7]. At the same time, gas is a clean energy source; if the released gas can be utilized reasonably during coal mining, it will reduce the risks associated with coal mines and improve the efficiency of clean energy utilization, protecting the environment. However, China's coal mines generally face challenges in gas management, and over 90% of the coal seams in high-gas mines are low-permeability coal seams^[8-9]. Therefore, research on gas management in coal mines and enhanced permeability technology for coal reservoirs is urgently needed.

After nearly decades of experimental exploration and field research, experts and scholars have proposed numerous methods to enhance coal reservoir permeability. Among these, traditional techniques such as hydraulic fracturing, hydraulic fracturing for fissure creation, and blasting for permeability enhancement stand out. Although current mainstream permeability enhancement measures for coal reservoirs have achieved some success in certain mines both domestically and internationally, given the complexity and diversity of China's coal geological conditions, these technologies exhibit certain limitations in practical application and are difficult to widely promote. Moreover, these technical means carry certain safety risks in actual operations and can easily damage the coal structure. Therefore, there is an urgent need for a new permeability enhancement technology for coal reservoirs that has a wide range of applicability, is easy to operate, low-cost, simple to manage, safe, reliable, and reusable.

In recent years, high-voltage pulse enhancement technology has emerged as an effective means to improve permeability in coal seams, increase gas extraction rates, and enhance the properties of coal reservoirs. This technology relies on the liquid-electric effect discovered by Yutkin. Through special circuit design, 220 V AC is stepped up and rectified into high-voltage DC, which is then stored in a pulse capacitor. The electrical energy is discharged into water, converting it into mechanical energy. By leveraging the weak compressibility of water to transfer energy, this process causes fracturing and modification of the coal rock mass under the influence of special electrodes connected between high and low voltage electrodes. The emergence of this innovative technology has provided new approaches for enhancing permeability in coal reservoirs. Building on this foundation, experts and scholars continue to delve deeper, tirelessly exploring further innovations in high-voltage pulse fracturing and enhancement technology^[10-13].

Zhao Lijuan^[14] conducted repeated electrical pulse fracturing experiments on coal to investigate the relationship between the number of fracturing cycles and the degree of pore-fracture derivation in coal. Li Hengle^[15-16] et al. found through high-pressure electrical pulse fracturing experiments that electrical pulse fracturing can effectively improve the pore and fracture structure of coal, enhance the connectivity between pores, increase the permeability of coal samples, and the width of macro-fractures shows a nonlinear increasing trend with the number of impacts. Liu Huanhuan [17] discovered during high-pressure pulse experiments in liquid water environments that the fracturing effect of high-voltage electrical pulses under static water pressure is much lower than its effect on injected water coal seams. That is, after performing high-pressure electrical pulse fracturing on coal samples in a liquid environment, the increase in pores and fractures is more significant. Jia Shaohua^[18] et al. established a high-pressure electrical pulse experimental platform in a liquid environment to investigate the relationship between discharge voltage, discharge time, and liquid pressure, finding that when the voltage is constant, the wavefront time increases continuously as the static water pressure increases. Yin Zhiqiang^[19] studied the changes in breakdown delay under different water pressure conditions, noting that the breakdown delay decreases gradually as the discharge voltage increases, while the peak current of the entire circuit continues to rise, exploring its feasibility for fracturing coal samples. The comparative study by Li Yi's team at Taiyuan University of Technology^[20-22] shows that the fracturing effect of electric pulses in liquid environments is superior to traditional hydraulic fracturing. The fracture parameters are positively correlated with discharge voltage, while static water pressure has a dual effect on shock waves: within the range of 0-5 MPa, the peak pressure of shock waves first increases and then decreases, which is related to the interaction between pressure constraining plasma channels and energy transfer efficiency. Xue Lexing^[23-25] et al. studied the influence of metal wires on energetic materials, and the results indicate that increasing the discharge voltage and the contact area of the metal wire can effectively enhance the initiation response intensity of molecular and ionic insensitive energetic materials. The initiation response intensity of molecular insensitive energetic materials is significantly affected, whereas ionic energetic materials are less sensitive to changes in plasma initiation conditions compared to molecular energetic materials.

2. EXPERIMENTS

2.1. Introduction to the Study Area

The Luanzhang Village Coal Mine is located in the Luan District of Changzhi City, Shanxi Province, at the southeastern edge of the Qishui Coalfield. The mining area is situated on the western slope of the Taihang Mountains, with an overall terrain that is higher in the northwest and lower in the southeast. The Quaternary strata in the region are relatively thin, and the exposure of bedrock is favorable, providing convenience for coal resource exploration and development. The mining area is located on the southeastern flank of the Qishui Syncline, with an overall structural form characterized by gentle monoclines, with a dip angle of 5°-15°. Major structural features include: Fault structures: mainly composed of medium and small normal faults, such as the F1 fault (strike NE, drop 10-20 meters), which has some impact on coal seam continuity. Fold structures: secondary gentle folds are well-developed, forming small anticlines or synclines locally, without causing significant damage to coal seam mining. Subsidence columns: karst development in Ordovician limestone has led to the formation of subsidence columns locally, requiring enhanced exploration during mining. The Shanxi Formation (P1s) contains coal-bearing strata with a thickness of about 60-80 meters, including the No.3 coal seam, which is the main coal seam mined in the area, averaging 5.5 meters in thickness and having a simple structure, classified as a stable coal seam. The coal type ranges from lean coal (PM) to thin coal (SM), with ash content ranging from 15%-20%, sulfur content from 0.5%-1.2%, and calorific value from 25-28 MJ/kg.

2.2. Sample Preparation

The coal seam in Lu 'an mining area was sampled, and fresh lump coal samples were collected and sealed in the working face according to the national standards GB/T19222-2003 and GB/T16773-2008.

Preparation of high pressure mercury intrusion test samples: Transport the large sample to the laboratory, and break the remaining coal block with a hammer to make it into 1~2cm³ coal block, and prepare several samples.

Table 1. Basic parameters of the coal samples

Proximate analysis (%)				Elemental analysis (%)				$R_{0, \max}$ (%)
M_{ad}	A_{ad}	V_{ad}	FC_{ad}	C_{daf}	H_{daf}	O_{daf}	N_{daf}	
1.35	7.48	13.68	65.72	87.40	3.94	2.27	1.07	2.1

M_{ad} : air-dry moisture content; A_{ad} : air-dry ash yield; V_{ad} : air-dry volatile matter; FC_{ad} : air-dry fixed carbon; C_{daf} : dry ash-free basis C; H_{daf} : dry ash-free basis H; O_{daf} : dry ash-free basis O; N_{daf} : dry ash-free basis N; $R_{0, \max}$: vitrinite maximum reflectance.

2.3. Experimental Procedure

In order to carry out the high voltage pulse experiment, a high voltage pulse experimental device was established. The experimental steps are as follows:

- (1) Connect the wire to the transducer window, and connect the transducer window to the power controller;
- (2) Place the energy-containing bullet in the transducer window to ensure that the energy-containing bullet will not fall off, and then put the energy-containing bullet into the pool;
- (3) Connect the power controller, capacitor and feeding mechanism in sequence, and connect the power control with 220 V power supply

(4) Debug the equipment to ensure that the instrument operates normally, and then carry out pulse test according to the predetermined scheme.

2.4. High pressure mercury injection

The high-pressure mercury porosimetry method is based on the theory of non-wetting phase seepage, utilizing the characteristic of high pressure driving mercury to break through capillary resistance in pores.

When pressure (p) exceeds the relationship between mercury surface tension (γ) and pore curvature radius (r) (following the $p = 2\cos\theta/r$ equation), the mercury phase gradually invades the pore system, and the pore size distribution characteristics can be reconstructed through the pressure-mercury influx function relationship.

The basic principle of high-pressure mercury porosimetry is that mercury does not wet most solids; the contact angle θ is typically greater than 90° (such as 140°), preventing mercury from spontaneously entering the pores.

External pressure must be applied to overcome the resistance caused by surface tension.

Mercury porosimetry quantitatively analyzes pore structure by controlling pressure, making it suitable for studying the pore size distribution of porous materials.

$$p = \frac{2\sigma \cos \theta}{r} \quad (1)$$

In the formula, P_c represents capillary pressure, MPa; σ is the interfacial tension between mercury and air, with a value of 0.480N/m ; θ is the wetting angle between mercury and coal, with a value of 140° , and r is the pore radius, μm .



Figure 1. AutoPore IV 9510mercury porosimeter

2.5. Low temperature liquid nitrogen experiment

The low-temperature liquid nitrogen adsorption method is a pore characterization technique based on the principle of physical adsorption. Its core mechanism and experimental methods are as follows: At liquid nitrogen temperature (77 K), nitrogen molecules physically adsorb onto solid surfaces through van der Waals forces. The adsorption capacity is regulated by relative pressure (P/P_0), which reflects the coverage of nitrogen molecules on the material surface. By measuring the nitrogen adsorption at different P/P_0 values, isotherms for adsorption and desorption can be plotted. Using BET theory, specific surface area can be calculated, and the pore size distribution can be derived using the Kelvin equation. The low-temperature liquid nitrogen adsorption method involves drying and degassing coal samples, then placing them in a liquid nitrogen environment. Nitrogen gas is introduced to achieve adsorption equilibrium, gradually adjusting the P/P_0 ratio, recording the equilibrium adsorption

amount, and heating to room temperature to complete desorption, recording the desorption amount. Based on the desorption curve, mesopores (2-50 nm) characteristics can be analyzed using the BJH model or DFT method. The experimental steps are as follows: (1) Nitrogen adsorption is carried out by Micromeritics AutoPore ASAP 2460 type adsorption instrument, and the coal sample is first heated and vacuum degassed to remove impurity gases adsorbed on the surface of the coal sample; (2) Then weigh and place it in liquid nitrogen. At the low temperature of liquid nitrogen, the nitrogen adsorption amount of the sample is measured at different pressure points preset, and the adsorption isotherm line is obtained. (3) The experimental data were analyzed to obtain the specific surface area, pore volume and pore size distribution of coal samples.

3. ANALYSIS

3.1. Analysis of high-pressure mercury injection loop

As shown in the figure, the mercury entry and exit curves of the original coal sample from Zhangcun basically overlap. The original coal sample contains a large number of sealed pores at one end, leading to poor pore connectivity. Compared with the original coal sample, after electro-pulse fracturing, the mercury entry and exit curves no longer overlap, and under the same pore size, the mercury exit curve always remains above the mercury entry curve. From Figure 2, it can be seen that before and after electro-pulse fracturing, during the initial mercury entry stage, as the mercury entry pressure increases, the mercury entry curve rises sharply without an accompanying mercury exit curve above it, with pore sizes ranging >10,000 nm. This indicates that the pore structure of the Zhangcun coal sample contains abundant open pores, semi-enclosed pores, and numerous fractures at this stage.

After electro-pulse fracturing, micro-pores and small pores with pore sizes between 10 nm and 100 nm in a semi-enclosed state become medium and large pores, leading to an increasing trend in the total pore volume of the coal sample, thereby enhancing the macroscopic pore connectivity of the coal sample.

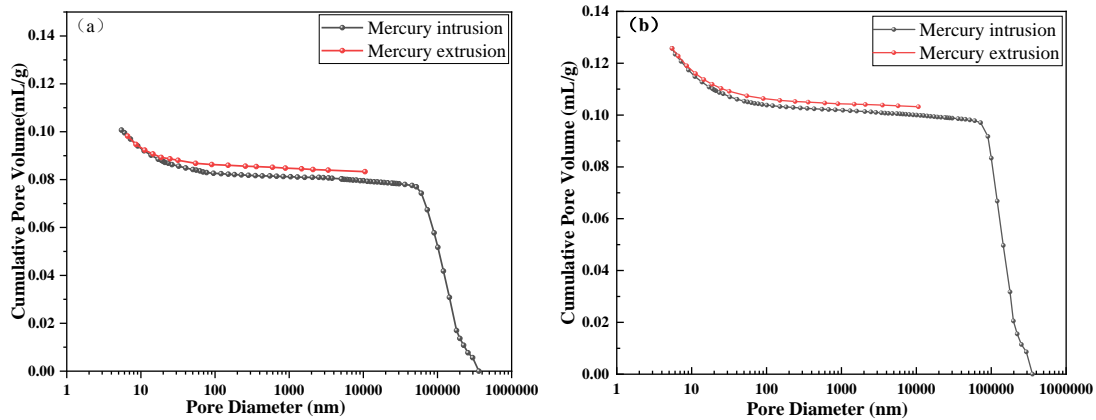


Figure 2. Mercury curve before and after fracturing of coal samples in Zhangcun:(a) ZC-0; (b) ZC-1

In order to study and compare the pore changes of coal samples caused by electric pulse more deeply, this paper studies.

The classification method of B.B. Hoddot was adopted to distinguish pore sizes, dividing the internal pores of coal samples into four parts: large pores (>1000 nm), medium pores (100 nm-1000 nm), small pores (10 nm-100 nm), and micropores (<10 nm). We analyzed the changes in porosity at various pore size intervals in both the original coal sample and the sample subjected to electric pulse fracturing impact. The total porosity of the original Zhangcun coal sample reached 0.1007 cm³/g, with large pores being the most significant, accounting for 80.63% of the total porosity at 0.0812

cm³/g. Medium pores accounted for 1.16% at 0.00120 cm³/g, small pores for 4.89% at 0.0094 cm³/g, and micropores for 9.29% at 0.0066 cm³/g. Small and medium pores correspond to diffusion pores and seepage pores, respectively, which together account for only 6.57% of the total porosity, indicating that the diffusion-seepage capability of the original Zhangcun coal sample is relatively weak.

After being subjected to electrical pulses, the total pore volume of the coal sample increased by 25.12% compared to the original coal sample; the macropore volume increased by 24.63%; the mesopore volume increased by 66.1%; the micropore volume increased by 16.39%; and the micro-pore volume increased by 12.10%. The total pore volume, compared to the original coal sample, has significantly increased, with the micropores and small pores accounting for 17.46% of the total pore volume, while the macropores and mesopores account for 82.54%. The reason for the increase in the total pore volume of the coal sample may be that the mesopores and macropores have significantly increased, while the micropores and micro-pores have only slightly increased. The significant increase in the macropores and mesopores is partly due to the destruction of semi-open pores during the fracturing process and the transformation of small and micro-pores into mesopores.

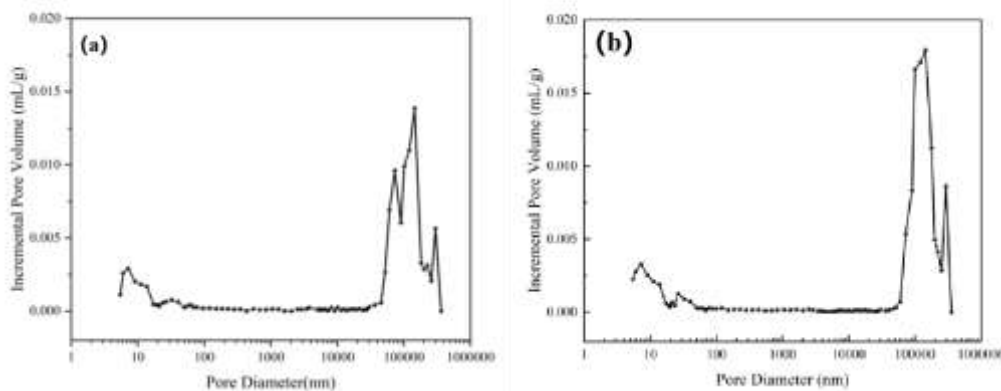


Figure 3. Changes in pore volume before and after fracturing of coal samples from Zhangcun: (a) ZC-0; (b) ZC-1

Table 1 shows the changes in pore volume and specific surface area of coal samples from Zhangcun after high-voltage electric pulse fracturing. Compared to the original coal samples, the specific surface areas of all stages of pore volume and specific surface area have changed after high-voltage electric pulse fracturing.

In gas adsorption theory, pore structure influences the adsorption, desorption, and migration processes of gases. The specific surface areas of small and micropores in coal samples are large, providing numerous adsorption sites for gas molecules. Therefore, the size of the specific surface areas of small and micropores significantly affects the adsorption capacity of coal samples. After high-voltage electric pulse fracturing, both the specific surface areas of small and micropores in coal samples have decreased to some extent, indicating that after fracturing modification, there are fewer sites available for gas molecules to adsorb, which is more conducive to the desorption and migration processes of gases.

The increase in the specific surface areas of large and mesopores suggests that after high-voltage electric pulse fracturing modification, shock waves act on the interior of the coal body, causing internal micro-fractures to continuously expand and connect. This change can increase the number of large and mesopores and may also improve pore connectivity, reducing the complexity within the pores. In summary, high-voltage electric pulse fracturing of coal samples leads to a decrease in the total specific surface area, a reduction in the specific surface areas of micropores and small pores, while the specific surface areas of large and mesopores increase to some extent.

Table 1. Changes of pore specific surface area in coal samples

number	S1	S2	S3	S4	ST	S1/ST	S2/ST	S3/ST	S4/ST
ZC-0	5.0829	1.9517	0.0349	0.0038	7.0701	71.85	27.58	0.50	0.053
ZC-1	4.8069	1.6479	0.0106	0.0090	6.4746	74.18	25.45	0.16	0.14

Note: ST is the total pore specific surface area; S1 is the micropore specific surface area; S2 is the small pore specific surface area; S3 is the mesopore specific surface area; S4 is the macropore specific surface area.

3.2. Analysis of low temperature liquid nitrogen data

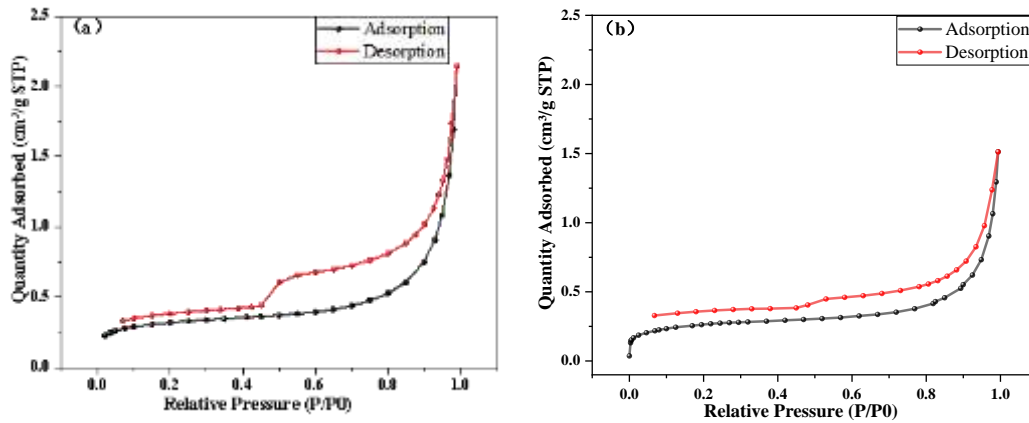


Figure 4. Low temperature liquid nitrogen adsorption curves before and after fracturing of coal samples in Zhangcun: (a) ZC-0; (b) ZC-1

The shape of the low-temperature liquid nitrogen adsorption loop of coal samples to some extent reflects the internal pore structure of the coal sample. The figure shows the low-temperature liquid nitrogen adsorption curves of raw coal samples from Zhangcun and Pingdingshan No.8 Mine before and after electro-pulse fracturing. As shown in Figure 4, whether it is the original coal sample or the coal sample modified by electro-pulse fracturing, its liquid nitrogen adsorption capacity increases with the increase in relative pressure, showing a positive correlation. When the relative pressure exceeds 0.9, the adsorption of nitrogen gas begins to increase rapidly. This indicates that there are large-scale pores within the coal sample, which can adsorb more nitrogen gas under high-pressure conditions. At a relative pressure of 0.5, the image of the original Zhangcun coal sample has a turning point, suggesting that there may be a fine-neck bottle-like (ink bottle-like) pore inside the coal sample. However, after electro-chemical composite energy pulse fracturing, the image of the Zhangcun coal sample at a relative pressure of 0.5 shows only a slight turning point, indicating that the fine-neck bottle-like (ink bottle-like) pores inside the coal sample have been effectively modified, and these pores gradually decrease in size as the relative pressure increases until they eventually disappear. This suggests that the complexity of the internal pores in the coal sample has decreased, and the porosity connectivity has gradually improved.

As shown in Figure 4, the nitrogen adsorption capacity of the original coal sample from Zhangcun reached $2.15 \text{ cm}^3/\text{g}$ when the relative pressure was 0.99. However, after electro-pulse fracturing treatment, the nitrogen adsorption capacity of the coal sample at a relative pressure of 0.99 significantly decreased to $1.58 \text{ cm}^3/\text{g}$, a reduction of 26.51%. This result indicates that the nitrogen adsorption capacity of the coal sample after fracturing treatment decreases.

Figure 5(a) and (b) show the pore size distribution of the original Zhangcun coal sample and the fractured coal sample based on low-temperature liquid nitrogen adsorption within the range of 1-100 nm. For the original Zhangcun coal sample, the total porosity and stage porosity change gradually between 1-10 nm. In the range of 10-100 nm, both the total porosity and stage porosity increase

rapidly with pore size. For the fractured coal sample, the growth is relatively stable between 1-5 nm, but it increases very quickly between 5-100 nm. The trend of the fractured coal sample is largely consistent with that of the original sample, although the pore size has changed.

The original Zhangcun coal sample had a pore volume of 0.00233 cm³/g, while the fractured coal sample had a pore volume of 0.00152 cm³/g, showing a certain degree of reduction.

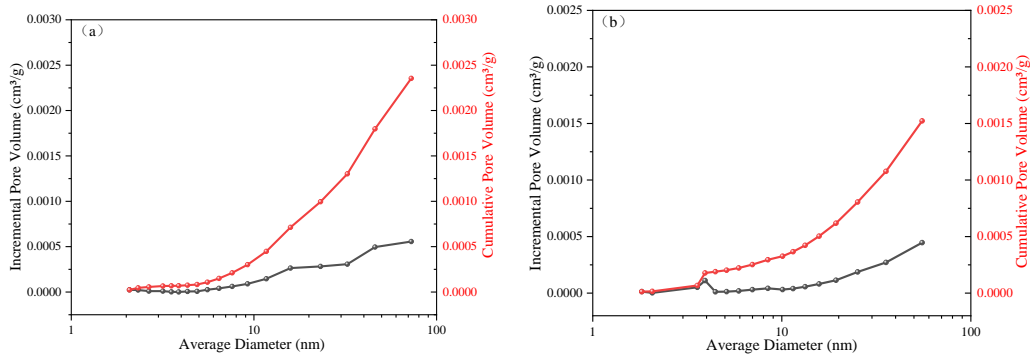


Figure 5. Comparison of pore volume before and after fracturing based on low temperature liquid nitrogen adsorption: (a) ZC-0; (b) ZC-1

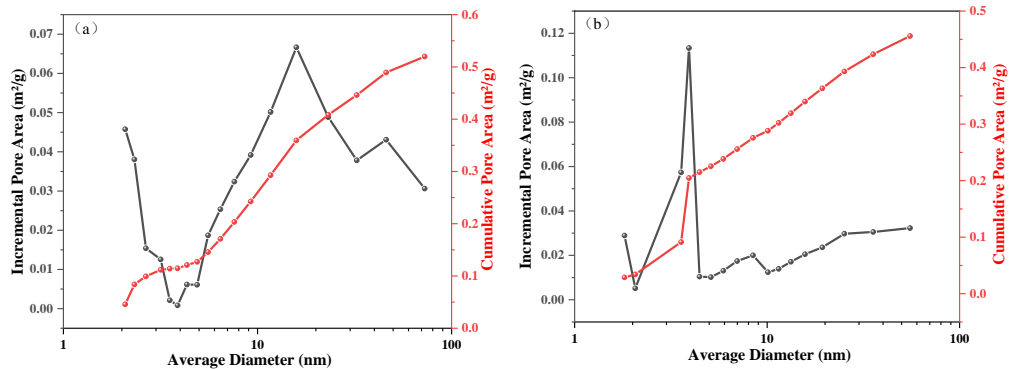


Figure 6. Comparison of specific surface area of coal samples before and after fracturing based on low temperature liquid nitrogen adsorption: (a) ZC-0; (b) ZC-1

Figure 6 (a) and (b) show the variation of internal porosity and specific surface area of Zhangcun coal samples. It can be seen from the figure that the total specific surface area of the original Zhangcun coal samples is 0.548652 m²/g, and the total specific surface area of the Zhangcun coal samples after fracturing transformation is 0.455894 m²/g, which is 16.94% lower than that of the original Zhangcun coal samples.

Table 2. Mesoporous structure parameters of coal samples

Number	Average mesopore diameter /nm	Mesopore volume (cm ³ /g)	Mesopore specific surface area (m ² /g)
ZC-0	25.41	0.0017	0.443
ZC-1	26.50	0.0007	0.251

4. CONCLUSIONS

High-voltage pulse fracturing is considered an effective method for enhancing permeability in coal seams, increasing gas extraction rates, and improving the pore structure of coal reservoirs. It has advantages such as easy operation, low cost, simple management, safety, reliability, and reusability. The main research findings are as follows:

(1) High-pressure mercury intrusion porosimetry data show that after high-voltage electrical pulse fracturing, the macroporosity and mesoporosity of Zhangcun coal samples increase, with the proportion of macropores and mesopores to total pore volume also increasing; overall, high-voltage electrical pulse fracturing leads to a significant increase in the size of macropore porosity in coal samples. This indicates that the impact wave of the electric pulse primarily modifies the meso- and macroporosity of the coal matrix.

(2) Low-temperature liquid nitrogen adsorption data show that high-voltage electric pulse fracturing reduces the liquid nitrogen adsorption capacity of Zhangcun coal samples, altering the internal pore morphology of the coal samples. The ink bottle pores in Zhangcun coal samples were effectively modified after fracturing.

Analysis of liquid nitrogen adsorption data indicates that after high-voltage electric pulse fracturing, the average pore size of mesopores in Zhangcun coal samples shows an increasing trend, while both pore volume and specific surface area decrease, indicating that the modified coal samples exhibit pore transformation phenomena.

REFERENCES

- [1] Yuan Liang. Carbon neutral development strategy of coal industry [J]. *Chinese Engineering Science*, 2023, 25(5): 103-110.
- [2] Gao Chao, Xu Nai Zhong, Liu Gui, et al. Challenges and Opportunities Facing the Development of China's Coal Industry [J]. *Coal Mine Mining*, 2019,24(1):1-4,29.
- [3] Bi Caiqin. China's coalbed methane resources and distribution [J]. *Petroleum Knowledge*, 2018(2): 12.
- [4] Yuan Liang. Challenges and Countermeasures for the High-quality Development of China's Coal Industry [J]. *China Coal*, 2020,46(1):6-12.
- [5] Wu Qiang, Tu Kun, Zeng Yifan, et al. Discussion on the main problems and countermeasures of upgrading China's main energy (coal) [J]. *Journal of Coal Science*, 2019,44(06):1625-1636.
- [6] Tang Yue. China's coalbed methane resources and prospects[C]//, Kunming, 2013:476-477.
- [7] Qin Yong. Progress and Review of China's Coalbed methane Geology Research [J]. *Journal of University Geology*, 2003, 9(3): 339-358.
- [8] Qin Yong, Shen Jian, Shi Rui. Strategic value and strategic choice of large-scale coalbed methane industry construction in China [J]. *Journal of Coal Science*, 2022,47(1):371-387.
- [9] Luo Pingya. Discussion on the substantial increase of single well production of coalbed methane Wells in China [J]. *Natural Gas Industry*, 2013,33(06):1-6.
- [10] Qin Yong, Qiu Aici, Zhang Yongmin. Experimental and exploration of new technology for coal reservoir enhancement by high energy repetitive strong pulse wave [J]. *Coal Science and Technology*, 2014(6): 1-7,70.
- [11] JIANG C B, WANG Y F, DUAN M K, et al. Experimental study on the evolution of pore-fracture structures and mechanism of permeability enhancement in coal under cyclic thermal shock[J]. *Fuel*,2021,304:121455.
- [12] JIANG C B, ZENG Y, DENG B Z, et al. Mechanisms underlying variations in pore structures and permeability in response to thermal treatment and their implications for underground coal utilization[J]. *Powder Technology*, 2024, 444: 120073.
- [13] ZHANG Di, ZHANG Yongmin, LI Jiandong, et al. Application of controllable shock wave seam permeability enhancement in cross seam drilling[J]. *Coal Engineering*,2023,55(6):73-78.
- [14] Zhao Lijuan, Wang Yadong, Zhang Meichen, et al. Adaptive cutting control strategy for coal mining machine under complex coal seam conditions [J]. *Journal of Coal Science*, 2022,47(1):541-563.
- [15] Li Hengle. Fracture and enhancement behavior of coal-rock electrical pulse stress wave and its mechanism [D]. *Geological Resources and Geological Engineering*, China University of Mining and Technology, 2015.
- [16] Li Hengle, Qin Yong, Zhou Xiaoting, et al. Development characteristics of micro-fractures in coal body under cyclic high voltage pulse action and its coal petrology control [J]. *Coalfield Geology and Exploration*, 2021,49(4):105-113.
- [17] Liu Huanhuan. Experimental study on desorption mechanism and permeability enhancement effect of low-permeability coalbed methane [D]. *School of Architecture and Civil Engineering*, Inner Mongolia University of Science and Technology, 2015.

- [18] Jia Shaohua, Zhao Jinchang, Yin Zhiqiang, et al. Study on the variation law of water shock wave front time based on high voltage pulse coal body permeability enhancement [J]. Journal of Taiyuan University of Technology, 2015(6):680-684,690.
- [19] Yin Zhiqiang. Study on the Electrohydraulic Properties of High Voltage Pulse Discharge in Water and Its Fracturing Effect on Coal Mass [D]. Mining Engineering, Taiyuan University of Technology, 2016.
- [20] Bao Xiankai, Jiang Bin, Zhang Wu, et al. Study on dynamic damage characteristics of coal and rock mass under shock wave pulsating load [J]. Coal Science and Technology, 2024,52(12): 204-223.
- [21] Yan D, Zhao J, Niu S, et al. Normal Reflection Characteristics of One-Dimensional Unsteady Flow Shock Waves on Rigid Walls from Pulse Discharge in Water[J]. Shock and Vibration, 2017,2017: 6958085.
- [22] Bian D, Zhao J, Niu S, et al. Rock Fracturing under Pulsed Discharge Homenergetic Water Shock Waves with Variable Characteristics and Combination Forms[J]. Shock and Vibration, 2018,2018: 6236953.
- [23] Xue Lexing, Wang Xiaofeng, Feng Xiaojun, et al. Detonation response of elemental explosives under plasma action [J]. Energy materials, 2017,25(1): 69-75.
- [24] Xue Lexing, Feng Xiaojun, Wang Xiaofeng. Research progress on the application of plasma technology in explosive detonation [J]. Journal of Fire and Explosives, 2017,40(1): 7-13.
- [25] Xue Lexing, Pan Wen, Feng Bo, et al. Influence of plasma ignition conditions on the response intensity of insensitive energetic materials [J]. Journal of Fire and Explosives Science, 2020,43(3):320-324.